



Technology and Instrumentation in Particle Physics 2011

An atomic layer deposition method to fabricate economical and robust large area microchannel plates for photodetectors

Anil U. Mane^{*a}, Qing Peng^a, Jeffrey W. Elam^a, Daniel C. Bennis^d, Christopher A. Craven^d, Michael A. Detarando^d, John R. Escolás^d, Henry J. Frisch^{a, b}, Slade J. Jokela^a, Jason McPhate^c, Michael J. Minot^d, Oswald H. W. Siegmund^c, Joseph M. Renaud^d, Robert G. Wagner^a, and Matthew J. Wetstein^{a, b}

^aArgonne National Laboratory, Argonne, Illinois 60439

^bEnrico Fermi Institute, University of Chicago, Chicago, Illinois 60637

^cSpace Sciences Laboratory, University of California, Berkeley, California 94720

^dIncom, Inc., Charlton, Massachusetts 01507

Abstract

We demonstrate an economical and robust route to fabricate large-area microchannel plate (MCP) detectors which will open new opportunities in larger area MCP-based detector technologies. Using our newly developed bottom-up process flow, we have fabricated large area MCPs (8"x8"). We used Atomic Layer Deposition (ALD), a powerful and precise thin film deposition technique, to tailor the electrical resistance and secondary electron emission (SEE) properties of large area, low cost, borosilicate glass capillary arrays. The self limiting growth mechanism in ALD allows atomic level control over the thickness and composition of resistive and secondary electron emission (SEE) layers that can be deposited conformally on high aspect ratio capillary glass arrays. We have developed several robust and reliable ALD processes for the resistive coatings and SEE layers to give us precise control over the resistance in the target range for MCPs (10^6 - $10^9\Omega$) and SEE coefficient (up to 8). The MCPs are tested in stacks of one or two plates and exhibit gains as high as 10^7 for a pair of MCPs. This approach allows the functionalization of microporous, insulating substrates to produce MCPs with high gain and low noise. These capabilities allow separation of the substrate material properties from the amplification properties. We studied the various MCP parameters such as gain, background counts, and resistance as a function of the ALD process parameters. Here we describe a complete process flow to produce fully functionalized working large area MCPs.

© 2011 Published by Elsevier Ltd. Selection and/or peer-review under responsibility of [name organizer]

Keywords: Atomic layer deposition, capillary arrays, microchannel plate, photodetector, secondary electron emission

^a Corresponding Author. Tel.: +1-630-252-7014

E-mail address: amane@anl.gov

1. Introduction

Microchannel plates (MCPs) are two dimensional arrays of microscopic channel electron multipliers. The scale-up of MCP-based detectors has been limited by the high cost and limited flexibility of existing MCP fabrication techniques. MCPs-based detectors can have a combination of unique properties such as high gain, high spatial resolution, high timing resolution, and very low background rate^[1-4]. MCPs can be used in a wide variety of detector applications including low-level signal detection, photo-detection, astronomy, electron microscopy, time-of-flight mass spectrometry, molecular and atomic collision studies, fluorescence imaging applications in biotechnology, field emission displays, and cluster physics^[1-7]. MCPs are also used to make visible light image intensifiers for night vision goggles and binoculars^[8]. The performance of MCP-based photodetectors depends not only on the microchannel plates themselves, but also on their configuration (e.g. single, double; chevron-type or triple; z-stack), as well as on the photocathode, the anode structure, and the signal readout. The Large Area Picosecond Photodetector (LAPPD) Project is a US Department of Energy (DOE) funded collaborative project^[9] that addresses each of these critical components of the photodetector with the goal of developing low cost, large area (8" x 8") MCP-based photodetectors. As part of the LAPPD project, our group^[10] is dedicated to achieving the batch production of workable MCPs derived from low cost glass capillary substrates.

The basic operation of an MCP is as follows: a negative bias potential is applied between the input and output electrodes to generate a uniform electric field along the pores of the MCP. An incident electron striking a pore wall near the input will induce emission of secondary electrons from the pore surface. These secondary electrons will be accelerated further along the pore by the bias potential, ultimately resulting in their collision with the pore wall. These also produce secondary electrons, resulting in an electron avalanche inside the pore and the emission of a cloud of electrons from the output of the pore. The amplification gain depends on the applied bias voltage. At typical voltages of ~1kV, the gain is in the range of 10^4 - 10^5 . The generation of secondary electrons is based on the incident electron energy, angle of incidence and the secondary electron emission (SEE) coefficient of the surface. The SEE yield is defined as the ratio of secondary electrons emitted to primary electrons incident on the surface. For practical reasons, MCPs are typically manufactured with intrinsic resistances in the range of 10-500M Ω , allowing the bias current to recharge electron depleted pores (post-avalanche) without drawing too much current (to prevent thermal over-heating and the need for large high voltage power supplies).

Conventional MCP fabrication process involves multi-fiber glass working techniques to draw, assemble, and etch an array of solid core fibers resulting in channels in a wafer of lead silicate glass. Additional thermo-chemical processing is used to activate the channel walls for electron multiplication. One of the drawbacks of MCPs made using this conventional process is that the electrical resistance and the secondary electron emission properties cannot be adjusted independently because both of these properties are imparted during the thermal activation step^[11]. Moreover, lead silicate glass is relatively expensive compared to borosilicate glass.

Recent progress in MCP readouts (multi-level architecture) and high speed electronic signal processing have allowed MCPs to be used in many applications more efficiently^[3, 12]. However, economical, larger area MCP manufacturing has not developed at the same pace. The increasing use of MCPs in various applications will require advances in MCP fabrication technology to reduce the manufacturing cost. Although several attempts have been made to produce MCPs with alternative processing strategies such as silicon micromachining^[13, 14] and lithographic etching of anodic alumina^[15], none of those technologies are mature enough to produce practical, large area MCPs. Recently, progress has been made to improve the MCP gain and performance by functionalizing conventional, non-activated MCPs with thin films^[2, 15]

. However, there are no detailed reports on economical, large area MCP fabrication which is the ultimate goal of the work described here.

This study is enabled by the convergence of two technical innovations. The first is the ability to produce large blocks of micro-capillary arrays being developed by Incom Inc. (Charlton, MA). The Incom process uses hollow, multifiber borosilicate (non-leaded) capillaries, eliminating the need to remove core material by chemical etching. The capillary arrays are fabricated as large blocks that are sliced to form large area wafers, without regard to the conventional limits of L/d (capillary length / pore diameter). The following steps are involved in fabricating borosilicate glass multifiber micro-capillary arrays: a) A single glass tube is heated and drawn under tension to form a hollow capillary; b) Multiple glass capillaries are assembled to form a hexagonal assembly which is heated and drawn to form a multi-capillary bundle; c) Multi-capillary, hexagonal-shaped bundles are further assembled and heated under pressure to form a fused block; d) The fused block is sliced into wafers having the desired dimensions and finished (ground, polished, and cleaned) to form the capillary array substrate. The second innovation is the advent of atomic layer deposition (ALD) coating methods to functionalize the capillary wafers described above.

The schematic of an MCP single pore prepared using our fabrication route is given in Figure 1. The resistive layer is applied first on borosilicate glass capillary substrate using an ALD process designed to synthesize films with the desired electrical resistivity. The SEE layer is applied next using a second ALD process selected to generate films with the desired SEE. This novel approach allows the resistive and emissive properties to be independently tuned^[16] and facilitates the functionalization of microporous, insulating substrates to produce MCPs^[2].

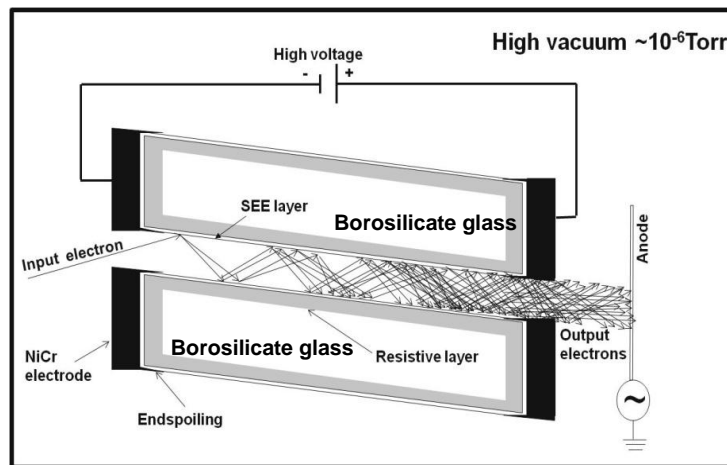


Figure 1(b). Schematic showing basic operation of single pore of an ALD-functionalized MCP with separate resistive and secondary electron emissive layers deposited on a borosilicate micro-capillary array

The progress in thin film deposition technology, nanomaterials engineering, and rigorous process flow controls stimulated by semiconductor manufacturing offer the opportunity to improve the performance and reduce the manufacturing cost of MCP-based devices. Among the various thin film processes, we have selected ALD for functionalizing the glass capillary arrays as a route towards cost effective MCPs. ALD provides exquisite thickness control and conformality (uniformity over complex, 3D surfaces) through the implementation of sequential, self-limiting surface reactions between gaseous chemical precursors and a solid surface. This process deposits films in an atomic layer-by-layer fashion and yields monolayer-level thickness and composition control as well as continuous, pinhole-free films^[16, 17]. The self-limiting aspect of ALD, coupled with gaseous diffusion of the precursor vapours, leads to excellent step coverage and highly conformal deposition even on very high aspect ratio structures^[18, 19]. Because the surface reactions are performed sequentially, the two precursors are never mixed in the gas phase. This separation of the two reactants eliminates possible gas phase reactions that can form particles that could deposit on the surface to produce granular films^[17]. ALD processing is also extendible to very large substrates and batch processing of multiple substrates^[20]. All of these capabilities are important for fabricating clean, batch-to-batch reproducible, economical, fully functionalized large area MCPs.

In this paper we describe a route to produce large area MCPs. Although this process flow could potentially be applied to a wide range of microchannel array substrates, here we have selected glass capillary arrays comprised of non-leaded borosilicate glass because this substrate has the potential to be manufactured in large sections at low cost.

2. Experimental

For the MCP development work we used 33 mm diameter glass micro-capillary array discs with thickness $L = 1.2$ mm, pore size $d = 20$ μm , aspect ratio $L/d = 60$, bias angle = 8° , and open area ratio $\approx 60\%$ manufactured by Incom, Inc. Prior to ALD functionalization, the substrates were cleaned ultrasonically in acetone for 5min., followed by flushing with ultrahigh purity (99.999%) nitrogen (20psi) for 30s. The cleaned MCP substrates were placed on a custom aluminium channel tray with minimum contact prior to ALD coating. Silicon coupons were also loaded along with the substrates for thickness monitors in a custom made tubular, hot-walled ALD reactor^[21]. We have developed proprietary ALD processes for synthesizing resistive coatings^[22]. These processes are based on blending, at the atomic scale, insulating and conducting materials in the appropriate ratio to achieve a target resistivity as has been demonstrated previously^[16]. The composition, and hence resistivity, of the film is dictated by the ratio of insulating and conducting components in the film. This ratio can be controlled by adjusting the relative number of ALD cycles performed to deposit the insulating and conducting components which is termed the precursor ratio. Among the several ALD resistive layers we have developed, the results discussed here are for the two best-performing ALD resistive processes (hereafter named “Chem-1” and “Chem-2”). In this study we also investigated two secondary electron emission (SEE) materials, ALD Al_2O_3 and MgO . All of the ALD layers in this study were amorphous as deposited according to X-ray diffraction (XRD) analysis. The experimental conditions for the ALD processing are summarized in Table 1. Photographs of an MCP at various process steps are shown in Figure 2(a-c).

The thicknesses of the resistive and SEE layers were determined using spectroscopic ellipsometry measurements on the Si monitor coupons. The conformality of the resistive layer coatings inside the MCP channels was examined by cross-sectional scanning electron microscopy (SEM). To facilitate electrical characterization, both sides of the MCPs were coated with 200 nm NiCr by evaporating 99.999% purity NiCr under 10^{-7} Torr vacuum as described below. During evaporation, the MCP(s) was mounted such that the pore axis was aligned at 45° with respect to the NiCr evaporation source on a rotating holder.

Consequently, each of the pores served as a shadow mask such that the NiCr electrode penetrated by one hole diameter into each pore (end-spoiling=1). The end-spoiling was confirmed by cross-sectional SEM. The MCP resistances were measured in vacuum (10^{-3} - 10^{-6} Torr) using a Keithley Model 6487 Picoammeter/Voltage Source. Feasibility, process margin in terms of resistance of the layer, and repeatability of the ALD processes were tested on several batches of MCPs. Repetitive current–voltage (I-V) behaviour, long term stability, and batch-to batch resistance reproducibility were also evaluated. The MCP gain and spatial uniformity, and the MCP lifetime via charge extraction for >6 months were measured in a high vacuum system equipped with a phosphor screen^[25].

Table1. ALD experimental parameters used for resistive and SEE coatings

Items	ALD Resistive layer		ALD SEE layer	
	Deposition temperature (°C)	200-300	200	200-300
ALD Chemistry	“Chem-1”	“Chem-2”	Al ₂ O ₃ using TMA/H ₂ O	MgO using Mg(Cp) ₂ /H ₂ O
Layer thickness (nm)	65	80	6	8
Growth monitor coupons	Si(100), fused quartz, MCPs	Si(100), fused quartz, MCPs	Si(100)	Si(100)
XRD analysis	amorphous	amorphous	amorphous	amorphous

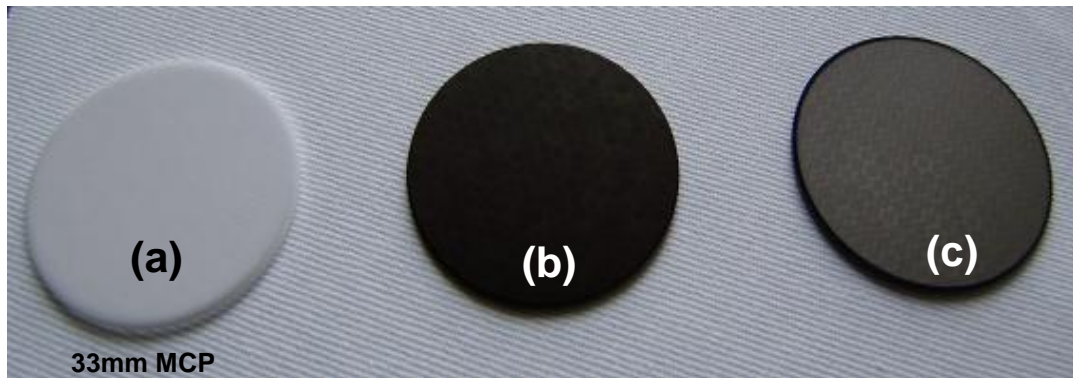


Figure 2. Photograph of as received bare 33mm MCP from Incom Inc.(a), after ALD resistive + SEE layers (b) After 200nm NiCr thermal evaporated coating on ALD functionalized MCP(c)

3. Results and discussion

A detailed investigation of both ALD Chem-1 and Chem-2 processes was conducted using planar substrates as well as MCPs to characterize the resistivity, thickness uniformity, microstructure, and stability in air. We noticed that both of the ALD resistive processes behaved similarly except that the relationship between resistivity and precursor ratio was different for the two materials. Furthermore, both the MgO and Al₂O₃ emissive layers on both chemistries were evaluated. For simplicity, all of the tests reported in this manuscript used the Chem-2 resistive coating prepared using a precursor ratio of 8% and MgO as the SEE layer coatings unless specified otherwise. Figure 3(a) shows the thickness uniformity profile for a series of substrates coated with the ALD Chem-2 resistive layer prepared using an 8%

precursor ratio on Si(100) witness coupons along the flow axis of the tubular ALD reactor. Data are shown for films grown in four separate batches. The excellent thickness uniformity along the reactor profile in each batch ($950 \pm 10 \text{ \AA}$) and between batches ($950 \pm 15 \text{ \AA}$) argues strongly for the successful scale-up of this process. Three batches of 5 MCPs were coated along with the Si(100) coupons and the resistances of these MCPs were determined using current–voltage (I–V) measurements (Figure 3b). As with the thickness data, the resistance measurements also exhibit very good uniformity within each batch ($115 \pm 15 \text{ M}\Omega$) and between batches ($115 \pm 10 \text{ M}\Omega$). This uniformity and process reproducibility bode well for the scale-up and integration of this ALD process into the manufacturing of $8 \times 8''$ MCPs.

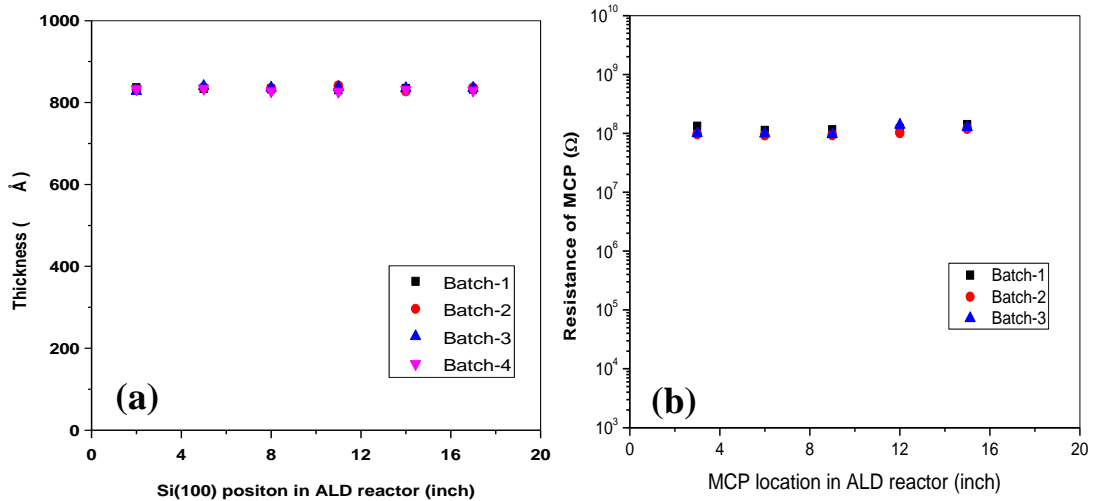


Figure 3. Thickness of Chem-2 resistive coatings prepared using a precursor ratio of 8% deposited on Si(100) substrates positioned along the flow-axis of the ALD reaction chamber for four identical deposition batches (a). Resistance of MCPs prepared along with the Si(100) substrates in three identical batches.

Figure 4(a) shows cross-sectional SEM images of an MCP coated with 835 \AA of the Chem-2 resistive layer. The higher magnification SEM images in the inset confirm that the deposited layer is conformal, uniform, and smooth along the pores of the MCP. The thickness measurements on the planar monitor Si(100) coupons by ellipsometry and from cross-section SEM of the MCP pore walls agree to within the 10% uncertainty of the SEM thickness measurements. The root mean squared (RMS) roughness of the resistive coatings inside of the pores was determined by atomic force microscopy (AFM) measurements (Figure 4b) to be $< 3\%$.

Fine-tuning of the ALD Chem-2 layer resistivity was accomplished by adjusting the ALD precursor ratio to control the relative proportion of conducting and insulating components of the film as shown in Figure 5(a) for quartz coupons and fully functionalized MCPs. During this set of experiments, all of the ALD process parameters were kept constant except for the precursor ratio. The film resistance on the quartz substrates was measured using a mercury probe contact ring method whereas the resistance on the MCPs was measured by contacting the NiCr electrodes and performing current–voltage (I–V) measurements. Under all conditions, a linear I–V response was obtained for the Chem-2 resistive layer over the voltage range 0–100V. The difference between the resistivities measured on the quartz substrates and the MCPs may result from deviations between the model geometry and true geometry for the capillary array

substrates, or from a slightly different composition inside of the high aspect ratio MCPs compared to the planar substrates. The predictable nature of the Chem-2 resistivity on the ALD precursor ratio allows the resistance of the MCPs to be tuned to optimize the steady-state current to suit a particular application. The resistivity of the Chem-2 layer is dependent on the ALD precursor ratio and this allows the resistance of the MCPs to be conveniently tuned to optimize the steady-state current to suit a particular application. The resistance stability of the 8% Chem-2 resistive layer on an MCP was tested under a constant 100V bias in vacuum at a pressure of $5e^{-6}$ Torr for over 1 week (Figure 5(b)). The MCP resistance was very stable during this test and exhibited only <5% resistance variations.

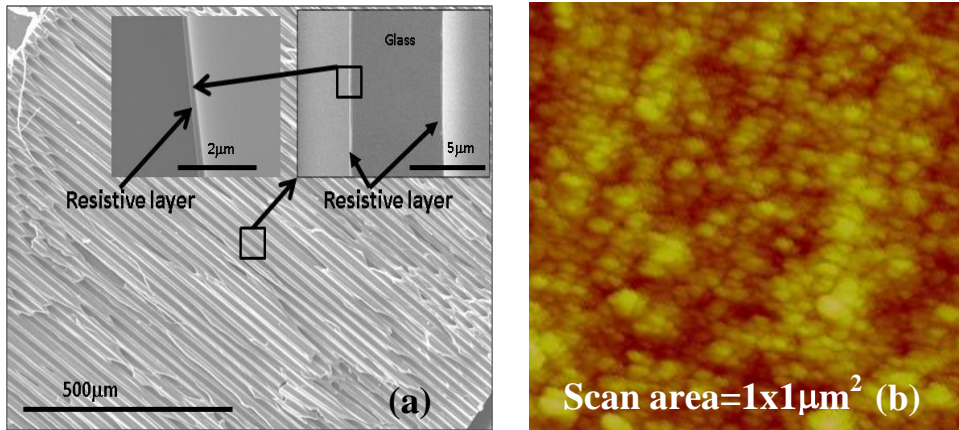


Figure 4. Cross-section SEM images taken from cleaved MCP coated with ALD Chem-2 resistive layer prepared using 8% precursor ratio (a) and AFM image acquired from inside surface of coated pore wall.

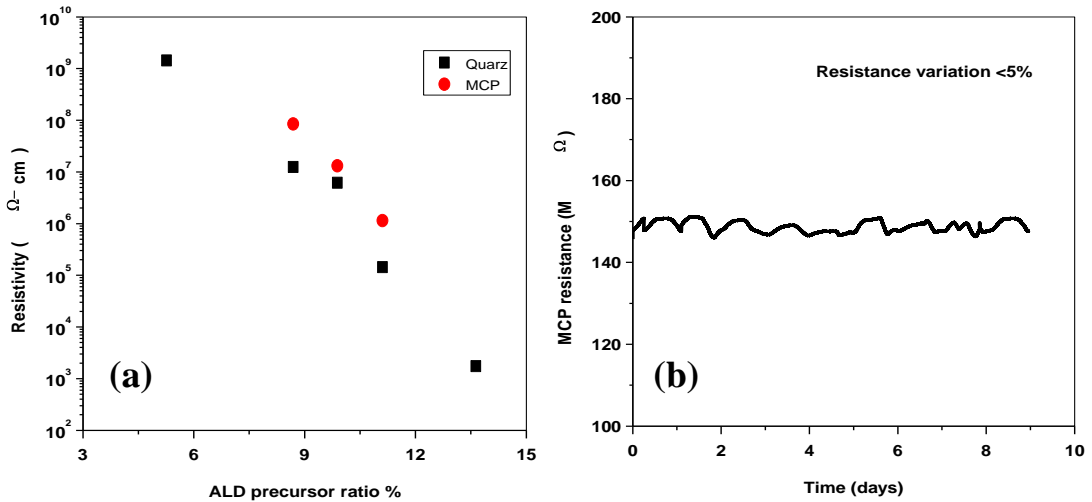


Figure 5. ALD Chem-2 layer resistivity vs. ALD precursor ratio (a); and MCP resistance stability vs. time under $5e^{-6}$ Torr vacuum for Chem-2 resistive layer prepared using 8% ALD precursor ratio (b).

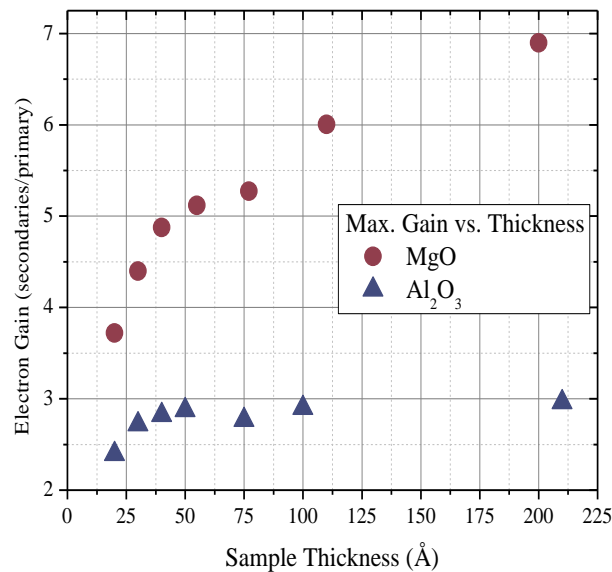


Figure 6. Maximum secondary electron yield vs. film thickness for ALD MgO and Al₂O₃.^[24]

The secondary electron coefficients for both the Al₂O₃ and MgO layers as a function of thickness (2–20nm) were studied in detail using X-ray- and ultraviolet-photoelectron spectrometry (XPS and UPS, respectively), and a low energy electron diffraction (LEED) module configured for SEE measurements as reported elsewhere^[24]. Figure 6 shows that the 6 nm ALD Al₂O₃ film gives an SEE yield of 3 whereas 8 nm ALD MgO gives an SEE yield of 5.5. In Al₂O₃, the maximum emission is reached with a film thickness of approximately 5nm. This corresponds to the maximum escape length for a secondary electron in this sample. Sample charging limited our ability to examine thicker samples of MgO^[24].

The gain and spatial uniformity of numerous fully functionalized MCPs were evaluated in a high vacuum system equipped with a calibrated electron source and a phosphor screen. The MCP gain with respect to applied voltage was examined and a sample data set for an MCP prepared using 935Å of the 8% Chem-2 resistive layer followed by 75Å of the MgO SEE layer is shown on a linear log plot in Figure 7(a). The gain increases exponentially at low voltages and then linearly in the saturated regime; at 1200V the gain is $>10^4$. This gain value is comparable to those obtained from commercial 33mm lead glass MCPs with a similar geometry. The phosphor screen image from the same MCP, Figure 7(b), demonstrates the uniformity of the performance of these ALD films. Overall, the phosphor image is fairly uniform in intensity and does not show any hot spots, areas of localized high background rate. The darker, hexagonal patterns visible in the phosphor image are caused by areas of lower gain attributed to pore crushing at the bond line interface between adjacent multi-capillary hexagonal bundles. The capillary glass fabrication process has been greatly improved since this device was evaluated and the pore deformations are now confined to one or two pores on either side of a multi-fiber boundary. The detailed electrical analyses of various MCPs are reported elsewhere^[20].

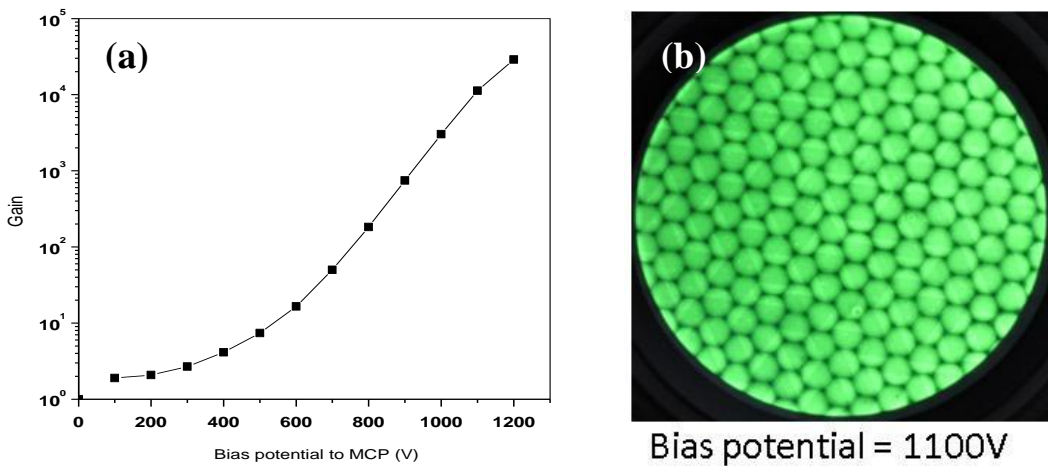


Figure 7. Gain vs. bias potential for MCP coated with 935Å 8% ALD Chem-2 resistive layer followed by 75Å MgO SEE layer (a); Phosphor image of same MCP under 1100V bias (b).

Lastly, we tested our optimized MCP fabrication process on 8"x8" glass capillary array plates fabricated using the same specifications as for the 33mm plates. Photographs of the as-received glass 8"x8" capillary substrate (a), after ALD functionalization using the Chem-1 resistive coating and Al₂O₃ SEE coating (b), and after 200nm NiCr electrode deposition by evaporation (c) are shown in Figure 8. The electrical analysis of this 8"x8" MCP was performed at UCB and details are reported elsewhere^[23]. The resistance of one of the 8"x8" MCPs was 3MΩ and exhibited electron multiplication similar to the 33 mm MCPs^[23]. Further work on large area MCP ALD processing and testing is in progress. We believe that the novel large area MCPs fabrication approach presented in this manuscript will offer an economical solution and open new opportunities for detector technology.

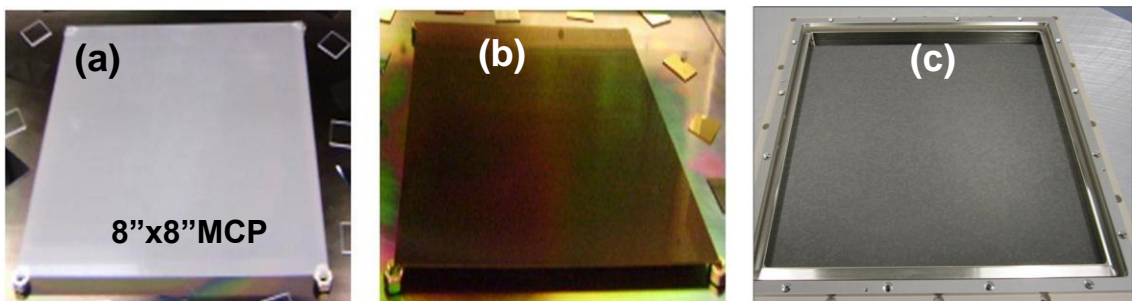


Figure 8. Photographs of the as-received 8"x8" glass capillary array substrate (a); after ALD functionalization using the Chem-1 resistive coating and Al₂O₃ SEE coating (b); and after 200nm NiCr electrode deposition on ALD functionalized plate (c).

4. Summary

We have demonstrated a process to fabricate large area MCPs. A newly developed ALD resistive layer shows conformal and uniform coating along the MCP pores and excellent reproducibility across multiple substrates and multiple batches. The characteristics of the resistive and SEE layers were tuned by adjusting the ALD process parameters such as temperature, composition, and precursor chemistry. Fully functionalized MCPs (33mm) fabricated by this method show good resistance stability, repeatable performance, uniform response, and gains comparable to commercial MCPs. We have demonstrated for the first time the functionalization by ALD of larger area (8"x8") MCPs.

Acknowledgements

The submitted manuscript has been created by UChicago Argonne, LLC, Operator of Argonne National Laboratory ("Argonne"). Argonne, a U.S. Department of Energy Office of Science laboratory, is operated under Contract No. DE-AC02-06CH11357. The U.S. Government retains for itself, and others acting on its behalf, a paid-up nonexclusive, irrevocable worldwide license in said article to reproduce, prepare derivative works, distribute copies to the public, and perform publicly and display publicly, by or on behalf of the Government. The authors would like to thank Eileen Hahn, (Fermi Lab) for the electrode deposition work, Hsien-Hau Wang for AFM analysis, and Electron microscopy was performed at the Electron Microscopy Centre at Argonne National Laboratory.

References

- [1] Siegmund, O. H. W.; Vallerga, J. V.; Tremsin, A. S., *Hubble's Science Legacy: Future Optical/Ultraviolet Astronomy from Space*, (2003) **291**, 403.
- [2] Beaulieu, D. R.; Gorelikov, D.; de Rouffignac, R.; Saadatmand, K.; Stenton, K.; Sullivan, N.; Tremsin, A. S., *Nuclear Instruments & Methods in Physics Research Section a-Accelerators Spectrometers Detectors and Associated Equipment*, (2009) **607**, 81.
- [3] Tremsin, A. S.; Pearson, J. F.; Fraser, G. W.; Feller, W. B.; White, P., *Nuclear Instruments & Methods in Physics Research Section a-Accelerators Spectrometers Detectors and Associated Equipment*, (1996) **379**, 139.
- [4] Wenzheng, Y.; Yonglin, B.; Baiyu, L.; Xiaohong, B.; Junping, Z.; Junjun, Q., *Nuclear Instruments & Methods in Physics Research, Section A (Accelerators, Spectrometers, Detectors and Associated Equipment)*, (2009), 291.
- [5] Morichev, I. E.; Pletneva, N. I., *Soviet Journal of Optical Technology/Soviet Journal of Optical Technology/Optiko-Mekhanicheskaya Promyshlennost*, (1974) **41**, ISSN 0038.
- [6] Suzuki, Y., *Journal of the Society of Photographic Science and Technology of Japan/Journal of the Society of Photographic Science and Technology of Japan*, (1986) **49**, 294.
- [7] Yang, W.-z.; Hou, X.; Bai, Y.-l.; Bai, X.-h.; Tian, J.-s.; Liu, B.-y.; Zhao, J.-p.; Qin, J.-j.; Ouyang, X., *Acta Photonica Sinica*, (2008), 439.
- [8] Thomas, N., *Image Intensifiers and Applications II*, (2000) **4128**, 54.
- [9] <http://psec.uchicago.edu>,
- [10] http://www.es.anl.gov/Energy_systems/Research/atomic_layer_deposition/index.html,
- [11] Wiza, J. L., *Nuclear Instruments & Methods*, (1979) **162**, 587.
- [12] Siegmund, O.; Tremsin, A.; Vallerga, J.; McPhate, J., *Nuclear Instruments & Methods in Physics Research Section a-Accelerators Spectrometers Detectors and Associated Equipment*, (2009) **610**, 118.
- [13] Tremsin, A. S.; Vallerga, J. V.; Siegmund, O. H. W.; Beetz, C. P.; Boerstler, R. W., *Future Euv/Uv and Visible Space Astrophysics Missions and Instrumentation*, (2003) **4854**, 215.
- [14] Xiaoming, C.; Jilei, L.; Ding, Y.; Pengliang, C.; Peisheng, X.; Shaohui, X.; Lianwei, W., *Journal of Micromechanics and Microengineering*, (2008), 037003.
- [15] Whikun, Y.; Taewon, J.; Sunghwan, J.; SeGi, Y.; Jeonghee, L.; Kim, J. M., *Review of Scientific Instruments/Review of Scientific Instruments*, (2000) **71**, 4165.
- [16] Elam, J. W.; Routkevitch, D.; George, S. M., *Journal of the Electrochemical Society*, (2003) **150**, G339.
- [17] George, S. M., *Chemical Reviews*, (2010) **110**, 111.
- [18] Elam, J. W.; Libera, J. A.; Huynh, T. H.; Feng, H.; Pellin, M. J., *J. Phys. Chem. C*, (2010) **114**, 17286.

- [19] Elam, J. W.; Xiong, G.; Han, C. Y.; Wang, H. H.; Birrell, J. P.; Welp, U.; Hryn, J. N.; Pellin, M. J.; Baumann, T. F.; Poco, J. F.; Satcher, J. H., Jr., *Journal of Nanomaterials*, (2006),
- [20] Granneman, E.; Fischer, P.; Pierreux, D.; Terhorst, H.; Zagwijn, P., *Surface & Coatings Technology*, (2007) **201**, 8899.
- [21] Elam, J. W.; Groner, M. D.; George, S. M., *Review of Scientific Instruments*, (2002) **73**, 2981.
- [22] Elam J. W., M. A. U., Peng Q., US patent application submitted, (2010).
- [23] Siegmund O.H.W., F. K., Hemphill R., Jelinsky S.R., McPhate J. B., Tremsin A.S., ; Vallerger J.V., F. H. J., Elam J. W., Mane A. U, Bennis D.C., Craven C.A., Deterando M.A., ; Escolas J.R., M. M. J., and Renaud J.M., (Submitted to Physics Procedia (2011).
- [24] Jokela Slade J., V. I. V., Zinoveva Alexander V., Elam Jeffrey W., Mane Anil U., Peng Qing, and Insepov Z., (Submitted to Physics Procedia (2011).